

Real-Time Image Segmentation via Hybrid Convolutional-Transformer Architecture Search

Hongyuan Yu, Cheng Wan, Mengchen Liu, Dongdong Chen, Bin Xiao, and Xiyang Dai[✉]

Abstract—Image segmentation is one of the most fundamental problems in computer vision and has drawn a lot of attentions due to its vast applications in image understanding and autonomous driving. However, designing effective and efficient segmentation neural architectures is a labor-intensive process that may require lots of trials by human experts. In this paper, we address the challenge of integrating multi-head self-attention into high resolution representation CNNs efficiently, by leveraging architecture search. Manually replacing convolution layers with multi-head self-attention is non-trivial due to the costly overhead in memory to maintain high resolution. By contrast, we develop a multi-target multi-branch supernet method, which not only fully utilizes the advantages of high-resolution features, but also finds the proper location for placing multi-head self-attention module. Our search algorithm is optimized towards multiple objective s (e.g., latency and mIoU) and capable of finding architectures on Pareto frontier with arbitrary number of branches in a single search. We further present a series of model via Hybrid Convolutional-Transformer Architecture Search (HyCTAS) method that searched for the best hybrid combination of light-weight convolution layers and memory-efficient self-attention layers between branches from different resolutions and fuse to high resolution for both efficiency and effectiveness. Extensive experiments demonstrate that HyCTAS outperforms previous methods on semantic segmentation task. Code and models are available at <https://github.com/MarvinYu1995/HyCTAS>.

I. INTRODUCTION

Image segmentation predicts pixel-level annotations of different semantic categories for an image. Different from image classification, which predicts a single label for the entire image, semantic segmentation performs pixel-level labeling with a set of object categories (e.g., sky, tree, human, car) for all image pixels. Image segmentation plays a crucial role in scene understanding such as medical image analysis [1], autonomous driving [2], [3], biometrics [4]–[6] and image understanding [6]–[8]. Thanks to the enormous successes of deep neural networks, recent segmentation networks [9]–[13] have achieved impressive progresses to generate high quality results with the utilization of high resolution representation learning in network design.

Recently, there are increasing interests in adapting self-attention mechanism [19] into vision tasks. Such self-attention modules can effectively model long-range dependencies and have been widely applied in natural language

H. Yu is with the Multimedia Department, Xiaomi Inc., Beijing 100085, China. (e-mail: yuhuan1995@gmail.com). H. Yu is also with the University of Chinese Academy of Sciences, Beijing 101408, China. C. Wan is with the School of Electrical and Computer Engineering, Georgia Institute of Technology, Atlanta 30332, USA. (e-mail: cwan38@gatech.edu). M. Liu, D. Chen, B. Xiao, and X. Dai are with Microsoft. (e-mail: {mengchliu, bin.xiao, xiyang.dai}@microsoft.com, cddlyf@gmail.com).

TABLE I: Comparisons with state-of-the-art search methods [14]–[18]. In which, ρ and τ represent the Pearson Correlation Coefficient and the Kendall Rank Correlation Coefficient of the true accuracy (by training each of them from scratch) and estimated accuracy (predicted by the super-network), **Memory Cost** reports the GPU memory consumption during the search process, **GPU Days** presents the searching cost, **Nums** reports the number of the number of the discovered architectures.

Method	GPU Days	Memory Cost	Nums	$\rho \uparrow$	$\tau \uparrow$
Auto-DeepLab [14]	3	Total supernet	1	0.31	0.21
FasterSeg [15]	2	Total supernet	1	0.35	0.25
SparseMask [16]	4.2	Total supernet	1	0.49	0.38
DPC [17]	2600	One subnet	1	0.46	0.37
Fast-NAS [18]	8	One subnet	1	0.42	0.33
HyCTAS(Ours)	5	One subnet	multiple	0.79	0.58

tasks. Although it provides an alluring alternative that solely relies on attention mechanisms, it is still far from mature to dispense convolution operators entirely because of the limitation of localization abilities due to insufficient low-level details. Hence, there is an imminent need to combine self-attention with high resolution representations.

However, naively replacing some convolution layers with self-attention layers is inefficient and non-trivial. There are two major aspects that cause the high computation cost. On one hand, the high resolution network requires to fuse features from multiple branches of different resolutions to effectively learn the semantics under various transformations. Such approaches often favor more on the prediction quality than the inference efficiency, thus resulting in heavy computation cost. For example, the latest variant of DeepLab [9] and HRNet [13] both run less than 5 FPS on a modern GPU, which is far from real-time applications. On the other hand, the network requires to maintain high-resolution representations through the whole process to generate accurate pixel-level prediction. Incorporating such resolution into self-attention layers will quadratically increase the computation cost. Due to above constraints and huge design space, manually designing effective and efficient high resolution networks with attention is a labor-intensive process that may require lots of trials from human experts.

In this paper, we propose a novel Hybrid Convolutional-Transformer Architecture Search (HyCTAS) framework to search for efficient networks with high-resolution representation and attention for superior image segmentation performance. We combine a light-weight convolution module to reduce the computation cost while preserving high-resolution

information and a memory efficient self-attention module to attend long-range dependencies. We search for an efficient architecture that not only fuses features from multiple levels but also maintains high-resolution representations from a multi-branch search space with different resolutions. Finally, we deploy an efficient genetic search algorithm that is optimized towards multiple objectives (i.e. latency, mIoU) and is capable of finding series of architectures on Pareto frontier with an arbitrary number of branches from different resolutions. Experiments demonstrate that our HyCTAS outperforms previous methods on semantic segmentation task.

Our main contributions are summarized as following:

- We design a novel searching framework incorporating with multi-branch space for high resolution representation and genetic-based multi-objective (e.g., latency and mIoU). We can obtain multiple networks covering both real-time speed and high precision within a single search at less than 5 GPU days.
- We present a series of HyCTAS that combines a light-weight convolution module to reduce the computation cost while preserving high-resolution information and a memory efficient self-attention module to attend long-range dependencies. Such combinations enable us to search for efficient architectures with high-resolution representations with attention.
- Extensive experiments on Cityscapes demonstrate better efficiency and effectiveness of the proposed approach over the state-of-the-art ones on semantic segmentation.

II. RELATED WORK

A. Efficient Networks for Image Segmentation

Semantic segmentation tasks, which aim to classify each pixel into predefined classes, have greatly benefited from the advancements in deep neural networks. Initially, the Fully Convolutional Neural Network (FCN) [20] illustrated the potential of convolutional neural networks in semantic segmentation by successfully applying them to this domain. Subsequently, the DeepLab [10] architecture introduced atrous convolution, enhancing the filters' field of view without an increase in parameters. Further improvements [9] were made by employing atrous convolution with varying atrous rates in a cascaded manner, optimizing the capture of multi-scale context. Most recently, HRNet [11], [12] was developed, which preserves high-resolution representations through the integration of high-to-low resolution convolutions and continuous fusions across parallel convolutions, leading to superior performance across various benchmarks.

While earlier segmentation methods have notably enhanced segmentation quality, the computational expense has often been overlooked, as seen in works such as those by [9], [13]. Efforts to mitigate computational costs while boosting inference speed have led to various innovations. [21] introduced a decoder network strategy to efficiently map low-resolution encoder feature maps back to the original input resolution, minimizing the necessity for high-resolution feature maintenance. [22] utilized a SqueezeNet-

inspired encoder with parallel dilated convolutions to enhance efficiency. [23] achieved real-time inference speeds by reducing feature map sizes early in the network. [24] developed ICNet, integrating multi-resolution input branches rather than feature-based ones to cut computational costs. More recently, [25] proposed the Bilateral Segmentation Network (BiSeNet), which employs a novel efficient design that separates a Spatial Path to retain spatial details and a Context Path to ensure an ample receptive field.

Unlike previous works, our proposed HyCTAS does not sacrifice any high-resolution feature maps to speedup, but intelligently searches for the most efficient combination of multi-resolution branches to find the both effective and efficient architecture.

B. Neural Architecture Search

Designing effective and efficient neural architectures is a labor-intensive process that may require lots of trials by human experts. Hence, automatic neural architecture search (NAS) has emerged in recent years. Based on the searching algorithms, existing NAS methods can also be roughly divided into two categories: gradient-based differentiable methods [26], [27] and sampling-based methods [28], [29].

Recent studies have applied NAS to image segmentation tasks. [30] were pioneers in utilizing NAS for designing a network architecture comprised of stacked computation cells for semantic image segmentation. [14] extended this by also searching for the network level structure, in addition to the cell level, to enhance segmentation. [15] introduced a method incorporating decoupled and fine-grained latency regularization to achieve a more favorable accuracy-latency trade-off. Most notably, [31] developed a framework capable of generating data-dependent routes to address scale variance in semantic representation by adapting to the scale distribution of each image.

Different from previous works, our method supports searching a combination of any number of multi-resolution branches, i.e. from 1/8 to 1/32, architectures to meet the needs of different scenarios. Compared with gradient-based differentiable methods, our proposed HyCTAS has the superiority in network capacity and higher performance with the budgeted resource consumption.

C. Transformer in Vision Tasks

Recently, there are two major directions in adopting transformer in vision tasks. One is the pure transformer architecture, the other is the hybrid architecture which combines the CNNs and the Transformer. Vision transformer [32] was the first full self-attention based Transformer architecture without CNNs, but had limitations to transfer to downstream tasks. Meanwhile, DETR [33] employed the hybrid model architecture, which combines the CNNs with Transformer. Later, SETR [34] adapted a similar idea of vision transformer to semantic segmentation. Although transformer allows us to model full-image contextual information, it is both memory and computation intensive. Many researchers [35], [36] intro-

TABLE II: The difference between typical operation and proposed efficient operation. Flops are measured using an input of size $1 \times 256 \times 32 \times 64$. The receptive field (RF) is relatively compared with the standard convolution.

Operation Type	Flops (G)	Params (M)	RF	Scale-to-Input
Convolution	1.2	0.59	1	Linear
Light-weight Convolution	0.4	0.66	2	Linear
Transformer	4.3	12.62	<i>Max</i>	Quadratic
Memory-efficient Self-attention	0.6	0.81	<i>Max</i>	Quadratic

duced trade-offs on speed and performance through manual designs, but have not achieved promising results yet.

In this paper, we also involve an efficient self-attention module as one basic component. Our proposed HyCTAS is automatically designed by setting two optimization goals (such as performance and latency) simultaneously and achieves state-of-the-art trade-off than handcrafted models.

III. PROPOSED APPROACH

A. Revisiting HRNet Architecture

Learning high-resolution representations is crucial to good performance on image segmentation. HRNet achieves this by maintaining **multi-branch** of convolution streams in parallel to maintain high-resolution representations through the whole network, and generates reliable high-resolution representations with strong position sensitivity through repeatedly fusing the representations from **multi-resolution** streams.

In order to preserve these two key properties, we design our HyCTAS supernet to enable searching for variant branch numbers, depths, widths, and spatial resolutions all in one. As shown in Figure 1, our supernet contains two types of searchable components: Cells and Nodes.

Given a supernet with L layers, after an input image going through the initial stem layers, the feature resolutions are downsampled to stride $S = \{1/8, 1/16, 1/32\}$ and fed into multiple searchable cells $C = \{C_s^1, C_s^1, \dots, C_s^L\}$. Then the features are fused into searchable nodes $N = \{N_s^1, N_s^1, \dots, C_s^{L-1}\}$ consecutively, where the cell and node are alternatively stacked. The searching domain is different for cell and node. A cell could contain multiple modules such as convolution, transformer and so on, which extends the network to be capable of combining **multi-module** into a sub-network; Meanwhile, a node is dedicated to fuse multiple branches from different resolutions together and behaves as a binary gate.

Since our architecture needs to support arbitrary branches fusion, which means the outputs of each architecture are not fixed, *i.e.*, the number of the last feature map channels and the branch position of the final outputs are not fixed. To solve these problems, we proposed a feature aggregation head module that can adapt to arbitrary output of different architectures. The feature map of shape $(C_* \times H \times W)$ is first adjusted in channels by a 1×1 Slimmable Convolution layer [37] to the shape of $(C_s \times H \times W)$. If the feature map size is not the max resolution in the search space,

it will be bilinearly upsampled to match the shape of the other feature map $(C_s \times 2H \times 2W)$. Then, two feature maps are concatenated and fused together with a 3×3 convolution layer. We enumerate all the output combinations and set a head for each type of output F_θ , so that there are a total of six different heads in our search space, *i.e.*, $\theta \in \{(8), (16), (32), (8, 16), (8, 32), (8, 16, 32)\}$.

Unlike previous works [14], [15] limits the network search to be one path, our HyCTAS supernet is cable of modeling sub-network with arbitrary number of branches from different resolutions, which better catches the spirit of HRNet.

B. Combing Multiple Modules

Convolutional operations enable the extraction of visual features through weight sharing, ensuring translation invariance while maintaining sensitivity to local image regions. However, this approach does not capture relative spatial relationships, leading to a constrained receptive field.

Achieving large receptive fields is essential for tracking long-range dependencies in images, typically necessitated by employing large kernels or multiple convolutional layers, albeit at an efficiency loss. Recent advancements leverage Transformer models [19] to efficiently address the constraints of convolutional methods.

Transformers employ multi-head self-attention to model inter-pixel importance across the entire input, achieving a maximized receptive field. However, compared to convolutional methods, transformers face significant computational challenges, particularly with large feature maps, as their computational and memory demands scale quadratically with input size.

Therefore, both operations do not meet our goal of pursuing efficiency if naively incorporated in our multi-resolution multi-branch framework for high resolution image segmentation learning. Hence, we propose to use a memory-efficient self-attention module and light-weight convolution module.

Memory-efficient Self-attention Module: Instead of directly borrowing typical transformer operation like previous works [38], we only employ the self-attention layer [39] without FFN to capture the glob context while maximize the efficiency. We then use the 1×1 convolutions for reducing and then increasing dimensions, leaving the self-attention module a bottleneck with smaller than input/output channels. This largely reduces the memory usages required in self-attention layer. Meanwhile, we add an extra bypassed 1×1 convolution module for preserving uncompressed residue.

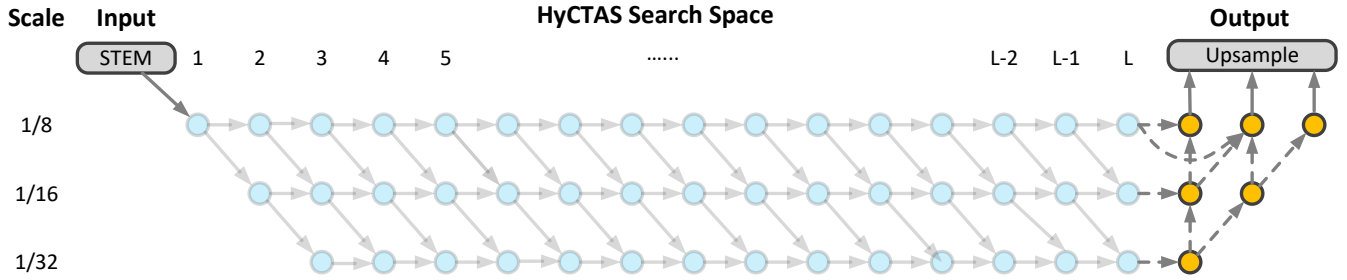


Fig. 1: An illustration of our HyCTAS search space. It preserves the multi-resolution and multi-branch proprieties of HRNet by introducing two types of searchable components: cells and nodes, which extend HRNet with multi-module fusion ability.

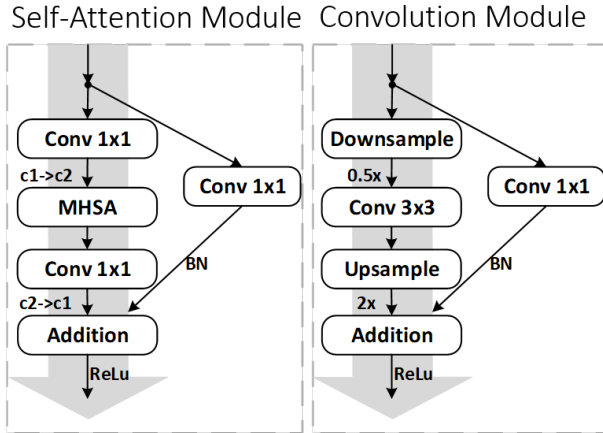


Fig. 2: An illustration of our searchable modules. We design a memory-efficient self-attention module and a light-weight convolution module and search for the best combination.

Our memory-efficient self-attention module operation can utilize the biggest receptive field, while keeping relatively small flops and memory footprint.

Light-weight Convolution Module: To maintain a large receptive field while minimizing computational costs, methods like Zoomed Convolution [15] and Dilated Convolution [9] employ bilinear sampling for input feature map resizing, inevitably leading to information loss. Addressing this, we introduce a novel, efficient convolution that incorporates a parallel 1×1 convolution to preserve high-resolution details as shown in Figure 2. This approach connects input feature map directly to the zoomed convolution’s output, effectively maintaining input resolution. Our lightweight convolution module significantly reduces information loss with minimal parameter increase, ensuring both speed and accuracy.

The detailed measurements of our memory-efficient self-attention module and light-weight convolution module are shown in Table 2. Meanwhile, properly combining convolutional module and self-attention module plays a significant role in the improvement of model performance and efficiency. Hence, we further deploy a search algorithm to solve this problem.

C. Searching with Multi-objective

Inspire by [40] and [41], we formulate the searching of the optimal architecture α^* as a two-stage optimization problem. The architecture search space \mathcal{A} is encoded in the supernet, denoted as $\mathcal{N}(\mathcal{A}, \mathcal{W})$. Each candidate architectures $\alpha \in \mathcal{A}$ share their weights across \mathcal{W} . In the first stage, we optimize the supernet weights \mathcal{W} by:

$$\mathcal{W} = \underset{\mathcal{W}}{\operatorname{arg\,min}} \mathcal{L}_{\operatorname{train}}(\mathcal{N}(\mathcal{A}, \mathcal{W})) \quad (1)$$

where $\mathcal{L}_{\operatorname{train}}$ denotes the training loss.

The prior distribution of $\Gamma(\mathcal{A})$ is important. In order to meet our goal of searching for architectures with arbitrary branch from different resolution, we pre-define this prior in the training process of the supernet. Since the sub-network with more branches contains the sub-network with less branches, we empirically set the sub-network with more branches to have a higher sampling probability.

$$\rho_i < \rho_{i+1}, i \in 1, 2, 3 \quad (2)$$

where ρ_i means the sampling of probability of architecture contains i branches. Other components in sub-network α are sampling from uniform distribution.

Once the supernet training is finished, the second-stage is to search for architectures via ranking the accuracy and latency of each sub-network $\alpha \in \mathcal{A}$. We convert the architecture searching problem to a standard multi-objective optimization (MOP) problem.

The formulation consists of decision variables, objective functions, and constraints. The optimization objectives are as follows:

$$\begin{aligned} \operatorname{Maximize} \quad & y = f(\alpha) = (f_1(\alpha), f_2(\alpha), \dots, f_k(\alpha)) \\ \operatorname{S.t.} \quad & e(x) = (e_1(\alpha), e_2(\alpha), \dots, e_m(\alpha)) \leq 0 \\ \operatorname{among} \quad & x = (\alpha_1, \alpha_2, \dots, \alpha_n) \in \mathcal{A} \\ & y = (y_1, y_2, \dots, y_k) \in Y \end{aligned} \quad (3)$$

Where α represents the decision vector, *i.e.*, the searched network architecture, y represents the target vector, *i.e.*, the mIoU and latency. \mathcal{A} represents the search space formed by the decision vector α , and Y represents the target space formed by the target vector y . And the constraint $e(x) \leq 0$ determines the feasible value range of the decision vector. In order to ensure that the searched architectures are effective, we set the following three constraints: 1) The number of

Algorithm 1 Multi-objective Search.

Input: supernet \mathcal{N} with weights \mathcal{W} , the number of branches b , the number of generations N , population size n , validation dataset D_{val} , objective weights w .

Output: K individual architectures on the Pareto front. Uniformly generate the populations P_0 and Q_0 until each has n individuals architectures.

for $i = 0$ **to** $N - 1$ **do**

$R_i = P_i \cup Q_i$

$F, S = \text{Non-Dominated-Sorting}(R_i)$

Pick n individual architectures to form P_{i+1} by ranks and the crowding distance weighted by w .

$Q_{i+1} = \emptyset$

while $\text{size}(Q_{i+1}) < n$ **do**

$M = \text{Tournament-Selection}(P_{i+1})$

$q_{i+1} = \text{Crossover}(M)$

if $\text{Latency}(q_{i+1}) > \text{Latency}(S_{max})$ **then**

continue

end if

Evaluate model q_{i+1} with S on D_{val}

if $mIoU(q_{i+1}) > mIoU_{min}$ **then**

Add q_{i+1} to Q_{i+1}

end if

end while

end for

Select the best performing architecture from Pareto-front from P_N on D_{val} .

paths in each sub-network needs to be greater than 0; 2) For a sub-network that contains multiple paths, the locations of down-sampling should be different; 3) In the down-sampling position, skip-connection cannot be selected; 4) The memory usage of a sub-network during training cannot exceed hardware limit.

Different from the Single-objective Optimization Problem, there is usually no unique optimal solution in MOP problem, but a Pareto optimal solution set. Hence, we adapt the popular evolution algorithm NSGA-II [42] to solve the optimization problem. The details of our searching algorithm can be found in the supplemental material.

The detail searching algorithm are presented in Algorithm 1. One-hot encoding is employed to encode the sub-network α . When the sampling is over, we will decode the sub-network to evaluate its corresponding mIoU and latency. We solve this multi-objective optimization (MOP) problem under the NSGA-II [42] framework.

IV. EXPERIMENTS

We evaluate our method on the semantic segmentation task.

A. Benchmark and Evaluation Metrics

Cityscapes [43] is a popular dataset which contains a diverse set of stereo video sequences recorded in street scenes from 50 different cities. It has 5,000 high quality pixel-level annotations. There are 2,975 images for training,

500 images for validation. And for testing, it offers 1,525 images without ground-truth for a fair comparison. The dense annotation contains 19 classes for each pixel.

Evaluation Metrics. The mean intersection over union per class (mIoU) and FPS (frame per second) are used as the metrics for semantic segmentation and speed, respectively.

B. Setup

Search. During training of the supernet, the sampling ratios for ρ_1 , ρ_2 and ρ_3 is set to 0.2, 0.3 and 0.5, respectively. The initial channel for supernet is 64 and the mini-batch size is set to 16. The supernet is trained on the Cityscapes dataset with 256×512 images on the training set. We use SGD optimizer with momentum 0.9 and weight decay of 5×10^{-4} to optimize the supernet weights. The learning rate is set to 0.02 with the exponential learning rate decay of 0.992. The entire supernet optimization takes about 120 hours on a single V100 GPU. In the search process, The initial population P_0 is set to 40 and generated by uniform random sampling. The probabilities of crossover and mutation operations are set at 0.9 and 0.02 respectively. Before the inference of a sub-network, the statistics of all the Batch Normalization [44] operations are recalculated on a random subset of training data (1000 images in Cityscapes). The number of generations is 20 and we search sub-networks with different branch numbers separately. Hence, a total of 2400 network sub-networks are searched.

Retrain. Similar to [14], we also use the filter multiplier to control the model capacity, and the default value for HyCTAS-S is set as 12, respectively. The final output stride of HyCTAS-S is 8 by merging the low level features in stem. We use SGD optimizer with momentum 0.9 and weight decay of 5×10^{-4} to optimize the searched networks. The 'poly' learning rate policy is employed with an initial learning rate of 0.005. Data augmentations on all datasets, *i.e.*, random crop, flipping etc., are consistent with [45]. On the Cityscapes dataset, the training images are cropped to 512×1024 and the mini batch size is set to 32. It is worth noting that all our results are trained from scratch without ImageNet pretraining and we only use the training set without any extra data.

Evaluation. We use Nvidia Geforce RTX 3090 and Intel Xeon E5-2680-v4 CPU (2.40GHz) for benchmarking the computation cost. When testing the inference speed, an image of a batch size of 1 is first loaded into the GPU memory and the model is warmed up to reach a steady speed. After that, the inference time is measured by running the model for six seconds. All the reported results, unless specified, are evaluated without multi-scale inference and flipping. The mean intersection over union per class (mIoU) is used as the evaluation metric for semantic segmentation.

C. Model Exploration

Our exploration focuses on balancing "Speed v.s. mIoU" in architecture search, highlighting how our framework excels in optimizing multiple objectives. Figure 3 shows architecture evolution, with color-coded branch numbers and

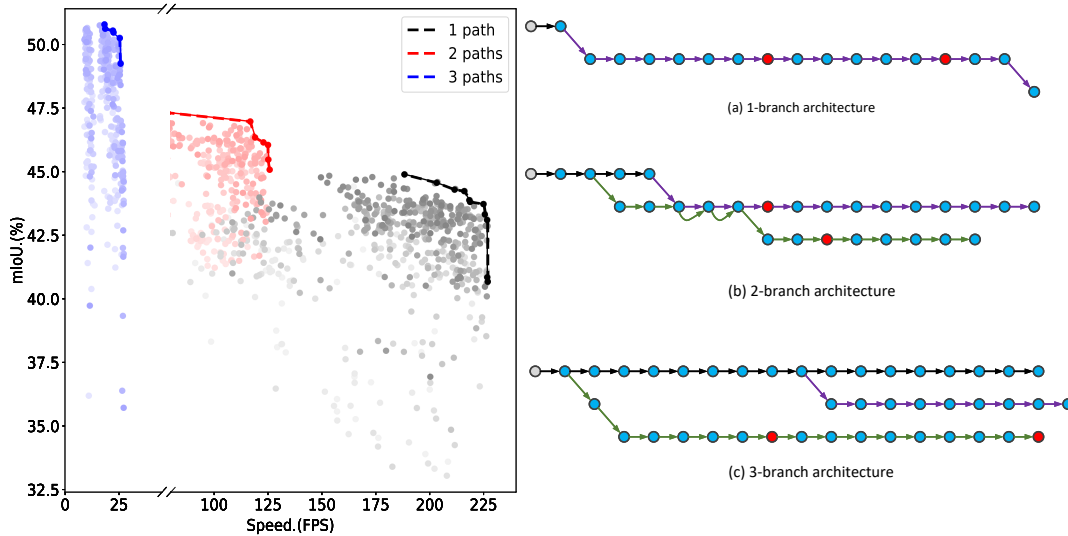


Fig. 3: An illustration of our searched architectures with multiple branches. The red dot indicates the location of the self attention module.

TABLE III: Comparison of semantic segmentation on the Cityscapes. †: speed on NVIDIA Xavier, ‡: speed with TensorRT acceleration, *: trained from scratch.

Methods	Input Size	mIoU (%) ↑ val	mIoU (%) ↑ test	Flops ↓ (G)	Params ↓ (M)	Speed ↑ (FPS)
ICNet [24]	1024x2048	67.7	69.5	-	-	37.7
BiSeNet [25]	768x1536	69.0	68.4	-	-	105.8
Fast-SCNN [46]	1024x2048	68.6	68.0	-	11.1	123.5
DF1-Seg-d8 [47]	1024x2048	72.4	71.4	-	-	136.9
HRNetV2 _{W18S} [12]	1024x2048	70.3	-	31.1	1.5	-
HRNetV2 _{W40} [12]	1024x2048	80.2	80.5	493.2	45.2	-
HyCTAS-S* (Ours)	1024x2048	72.3	73.0	13.0	1.5	159.2
CAS [30]	768x1536	71.6	70.5	-	-	108.0
MobilenetV3 [48]	-	72.4	72.6	9.7	1.5	10.8 [†]
SqueezeNAS [49]	-	73.6	72.5	19.6	1.9	10.2 [†]
FasterSeg [15]	1024x2048	73.1	71.5	28.2	4.4	149 [‡]
SeaFormer-S [50]	1024x2048	70.7	71.0	2.0	-	7.7
SeaFormer-B [50]	1024x2048	72.2	72.5	3.4	-	4.8
HyCTAS-M* (Ours)	1024x2048	77.1	75.7	29.4	2.4	87.8

a highlighted Pareto boundary at the search’s end, demonstrating the effect of dual-goal targeting on architecture distribution. We prioritize architectures on the Pareto frontier for their optimal balance and practical relevance.

We visualized searched architectures with varying branch numbers in Figure 3 (a)(b)(c), revealing interesting patterns in the placement of self-attention modules. With a single branch, self-attention is positioned at higher resolutions to enhance performance. Conversely, with three branches, self-attention is placed deeper to effectively fuse features across branches, aligning well with its strengths and limitations.

D. Comparison to SOTA

We compare our method with state-of-the-art methods on two popular benchmarks.

Cityscapes. Shown in Table III, we can see that when the speed is more than 100FPS, our model establishes new

state-of-the-arts. HyCTAS-M consistently outperforms recent BiSeNet [25], Fast-SCNN [46] and DF1-Seg-d8 [47]. In particular, our HyCTAS-M achieves 77.1% mIoU on Cityscapes validation set with 29.4G Flops and 2.4M parameters, which surpasses HRNetV2-W18-Small-v1 by 6.8% with similar model size. On the Cityscapes test set, our HyCTAS-M surpasses FasterSeg [15] by 4.2 %. Moreover, the speed of our model reaches an astonishing 87.8 FPS without TensorRT acceleration. Meanwhile, our HyCTAS-S has the smallest Flops and parameters and achieves the fastest inference speed at 159.2 FPS. This proves that our models are very competitive when deployed on real hardware.

Our method outperforms recent NAS models in search efficiency and GPU memory usage. Firstly, our multi-objective strategy allows HyCTAS to find models catering to varied needs, such as low latency or high performance, within just 5 GPU days. In contrast, traditional NAS methods

search for a single model at a time, leading to linearly increasing search costs with each additional model. Secondly, HyCTAS-M surpasses baseline NAS models in performance; for instance, it’s 3.8% better than FasterSeg [15] on the Cityscapes validation set.

These results are achieved with only Cityscapes fine-annotated images, without using any extra data (coarse-annotated images, COCO, ImageNet, etc.).

E. Ablation

Compared to Random Sampling. To evaluate our search strategy, we contrasted our architectures with 5 randomly sampled ones (1-3 branches) on the Cityscapes validation set. Table IV shows the average performance of these random architectures. Our discovered Searched-1 architecture surpasses its random counterpart by 4.3% in accuracy with a reduced model size. The discovered Searched-2 and Searched-3 both surpass random architectures by more than 3%.

Robustness of Searching. We further conduct an ablation study by intentionally changing components to verify the searching robustness on our HyCTAS-M model. Shown in Table V, we distort the searched architectures by replacing all self-attention to convolution, replacing all convolution to self-attention, shifting self-attention to another position and shifting self-attention to another branch, i.e. moved it to a random position on the same stride. It can be seen that our searched models consistently perform better these variants and proves its robustness.

In summary, the architecture searched by HyCTAS can find a great trade-off between performance, model size, and latency.

TABLE IV: Ablation study on the random sampled architectures on the Cityscapes validation set.

Architectures	Flops (G)	Params (M)	mIoU (%)
Random-1	14.6 ± 1.2	1.5 ± 0.2	68.0 ± 3.9
Searched-1	9.6	1.5	72.3
Random-2	31.6 ± 1.0	2.0 ± 0.7	73.6 ± 1.8
Searched-2	22.4	3.2	77.
Random-3	391.5 ± 11.4	32.0 ± 4.8	77.6 ± 0.9
Searched-3	335.1	43.2	80.9

TABLE V: Ablation study on the searched architectures on the Cityscapes validation set.

Architectures	Flops (G)	Params (M)	mIoU (%)
Searched	29.4	2.4	77.1
+ SA → Conv.	23.1	2.8	75.6
+ Conv. → SA	20.5	2.5	74.3
+ Shift SA Position	23.1	2.8	75.2
+ Shift SA Branch	22.5	2.6	75.6

Retrain Settings. From Table VI, we can see that adding the scheduled drop path [14], [51] improves the mIoU by 1.5%. When set the scheduled drop path probability to

TABLE VI: Experiments with different settings on Cityscapes validation set. ‘SDP’ denotes Scheduled Drop Path.

#	Iter-186k	Iter-372k	SDP-0.1	SDP-0.2	mIoU(%)
1	✓				71.5
2	✓		✓		73.0
3	✓			✓	73.3
4		✓		✓	73.5

0.2, the performance is improved by 0.3%. In #4, we also study the effects of bigger training iterations. Increasing the training iterations from 186K to 372K iterations, further improves the performance by 0.2%. All reported results are obtained without ImageNet [52] pretraining.

Correlation Analysis. We sampled 10 subnetworks, training each from scratch for 40,000 iterations. The results, shown in Table I, reveal a high correlation between the mIoU scores within the supernet and after retraining, with a Kendall’s τ of 0.58 and a Pearson Correlation Coefficient (ρ) of 0.79. This strong correlation confirms our ability to identify high-performing subnetworks within the supernet. Moreover, our search method not only reduces search and GPU memory costs compared to state-of-the-art methods but also efficiently yields multiple viable architectures from a single search process.

V. CONCLUSION

In this paper, we propose a novel HyCTAS framework to search for efficient networks with high-resolution representation and attention. We introduce a light-weight convolution module to reduce the computation cost while preserving high-resolution information and a memory efficient self-attention module to capture long-range dependency. By combing a multi-branch search space and an efficient genetic search algorithm with multiple objectives, our searched architectures not only fuse features from selective branches for efficiency, but also maintain high-resolution representations for performance. Besides, the discovered architecture also provides us with some insights into how to use self-attention when designing new networks. Extensive experiments demonstrate that HyCTAS outperforms previous methods on the semantic segmentation task, while significantly improving the inference speed. Future work will focus on applying this approach to more challenging tasks, such as key-point localization and object detection.

REFERENCES

- [1] E. H. Said, D. E. M. Nassar, G. Fahmy, and H. H. Ammar, “Teeth segmentation in digitized dental x-ray films using mathematical morphology,” *IEEE transactions on information forensics and security*, vol. 1, no. 2, pp. 178–189, 2006.
- [2] Z. Sun, S. Balakrishnan, L. Su, A. Bhuyan, P. Wang, and C. Qiao, “Who is in control? practical physical layer attack and defense for mmwave-based sensing in autonomous vehicles,” *IEEE Transactions on Information Forensics and Security*, vol. 16, pp. 3199–3214, 2021.
- [3] K. Thanikasalam, C. Fookes, S. Sridharan, A. Ramanan, and A. Pini-diyaarachchi, “Target-specific siamese attention network for real-time object tracking,” *IEEE Transactions on Information Forensics and Security*, vol. 15, pp. 1276–1289, 2019.

- [4] C. Wang, J. Muhammad, Y. Wang, Z. He, and Z. Sun, "Towards complete and accurate iris segmentation using deep multi-task attention network for non-cooperative iris recognition," *IEEE Transactions on information forensics and security*, vol. 15, pp. 2944–2959, 2020.
- [5] M. Liu and P. Qian, "Automatic segmentation and enhancement of latent fingerprints using deep nested unets," *IEEE Transactions on Information Forensics and Security*, vol. 16, pp. 1709–1719, 2020.
- [6] C. Peng, N. Wang, J. Li, and X. Gao, "Soft semantic representation for cross-domain face recognition," *IEEE Transactions on Information Forensics and Security*, vol. 16, pp. 346–360, 2020.
- [7] S. He and L. Schomaker, "Fragnet: Writer identification using deep fragment networks," *IEEE Transactions on Information Forensics and Security*, vol. 15, pp. 3013–3022, 2020.
- [8] A. R. Lejbolle, K. Nasrollahi, B. Krogh, and T. B. Moeslund, "Person re-identification using spatial and layer-wise attention," *IEEE Transactions on Information Forensics and Security*, vol. 15, pp. 1216–1231, 2019.
- [9] L.-C. Chen, G. Papandreou, F. Schroff, and H. Adam, "Rethinking atrous convolution for semantic image segmentation," *arXiv:1706.05587*, 2017.
- [10] L.-C. Chen, G. Papandreou, I. Kokkinos, K. Murphy, and A. L. Yuille, "DeepLab: Semantic image segmentation with deep convolutional nets, atrous convolution, and fully connected crfs," *TPAMI*, 2019.
- [11] K. Sun, Y. Zhao, B. Jiang, T. Cheng, B. Xiao, D. Liu, Y. Mu, X. Wang, W. Liu, and J. Wang, "High-resolution representations for labeling pixels and regions," *arXiv:1904.04514*, 2019.
- [12] J. Wang, K. Sun, T. Cheng, B. Jiang, C. Deng, Y. Zhao, D. Liu, Y. Mu, M. Tan, X. Wang, W. Liu, and B. Xiao, "Deep high-resolution representation learning for visual recognition," *TPAMI*, 2019.
- [13] B. Cheng, B. Xiao, J. Wang, H. Shi, T. Huang, and L. Zhang, "High-erhnet: Scale-aware representation learning for bottom-up human pose estimation," *2020 IEEE/CVF Conference on Computer Vision and Pattern Recognition (CVPR)*, pp. 5385–5394, 2020.
- [14] C. Liu, L.-C. Chen, F. Schroff, H. Adam, W. Hua, A. L. Yuille, and L. Fei-Fei, "Auto-deeplab: Hierarchical neural architecture search for semantic image segmentation," in *CVPR*, 2019.
- [15] "Fasterseg: Searching for faster real-time semantic segmentation," in *ICLR*, 2020.
- [16] H. Wu, J. Zhang, and K. Huang, "Sparsmask: Differentiable connectivity learning for dense image prediction," in *Proceedings of the IEEE/CVF International Conference on Computer Vision*, 2019, pp. 6768–6777.
- [17] L.-C. Chen, M. D. Collins, Y. Zhu, G. Papandreou, B. Zoph, F. Schroff, H. Adam, and J. Shlens, "Searching for efficient multi-scale architectures for dense image prediction," in *NeurIPS*, 2018.
- [18] V. Nekrasov, H. Chen, C. Shen, and I. Reid, "Fast neural architecture search of compact semantic segmentation models via auxiliary cells," in *Proceedings of the IEEE/CVF Conference on Computer Vision and Pattern Recognition*, 2019, pp. 9126–9135.
- [19] A. Vaswani, N. Shazeer, N. Parmar, J. Uszkoreit, L. Jones, A. N. Gomez, L. Kaiser, and I. Polosukhin, "Attention is all you need," in *NIPS*, 2017.
- [20] J. Long, E. Shelhamer, and T. Darrell, "Fully convolutional networks for semantic segmentation," in *CVPR*, 2015.
- [21] V. Badrinarayanan, A. Kendall, and R. Cipolla, "Segnet: A deep convolutional encoder-decoder architecture for image segmentation," *TPAMI*, 2017.
- [22] M. Trembl, J. A. Arjona-Medina, T. Unterthiner, R. Durgesh, F. Friedmann, P. Schuberth, A. Mayr, M. Heusel, M. Hofmarcher, M. Widrich, B. Nessler, and S. Hochreiter, "Speeding up semantic segmentation for autonomous driving," 2016.
- [23] A. Paszke, A. Chaurasia, S. Kim, and E. E. Cukurciello, "A deep neural network architecture for real-time semantic segmentation," *arXiv preprint arXiv:1606.02147*, 2016.
- [24] H. Zhao, X. Qi, X. Shen, J. Shi, and J. Jia, "Icnet for real-time semantic segmentation on high-resolution images," in *ECCV*, 2018.
- [25] C. Yu, J. Wang, C. Peng, C. Gao, G. Yu, and N. Sang, "Bisenet: Bilateral segmentation network for real-time semantic segmentation," in *ECCV*, 2018.
- [26] H. Liu, K. Simonyan, and Y. Yang, "Darts: Differentiable architecture search," in *ICLR*, 2019.
- [27] S. Xie, H. Zheng, C. Liu, and L. Lin, "SNAS: stochastic neural architecture search," in *International Conference on Learning Representations*, 2019. [Online]. Available: <https://openreview.net/forum?id=rylqooRqK7>
- [28] E. Real, A. Aggarwal, Y. Huang, and Q. V. Le, "Regularized evolution for image classifier architecture search," in *Proceedings of the AAAI Conference on Artificial Intelligence*, vol. 33, 2019, pp. 4780–4789.
- [29] M. Tan, B. Chen, R. Pang, V. Vasudevan, M. Sandler, A. Howard, and Q. V. Le, "Mnasnet: Platform-aware neural architecture search for mobile," in *The IEEE Conference on Computer Vision and Pattern Recognition (CVPR)*, June 2019.
- [30] Y. Zhang, Z. Qiu, J. Liu, T. Yao, D. Liu, and T. Mei, "Customizable architecture search for semantic segmentation," in *CVPR*, 2019.
- [31] Y. Li, L. Song, Y. Chen, Z. Li, X. Zhang, X. Wang, and J. Sun, "Learning dynamic routing for semantic segmentation," in *CVPR*, 2020.
- [32] A. Dosovitskiy, L. Beyer, A. Kolesnikov, D. Weissenborn, X. Zhai, T. Unterthiner, M. Dehghani, M. Minderer, G. Heigold, S. Gelly, J. Uszkoreit, and N. Houlsby, "An image is worth 16x16 words: Transformers for image recognition at scale," *arXiv preprint arXiv:2010.11929*, 2020.
- [33] N. Carion, F. Massa, G. Synnaeve, N. Usunier, A. Kirillov, and S. Zagoruyko, "End-to-end object detection with transformers," in *European Conference on Computer Vision*. Springer, 2020, pp. 213–229.
- [34] S. Zheng, J. Lu, H. Zhao, X. Zhu, Z. Luo, Y. Wang, Y. Fu, J. Feng, T. Xiang, P. H. Torr, et al., "Rethinking semantic segmentation from a sequence-to-sequence perspective with transformers," *arXiv preprint arXiv:2012.15840*, 2020.
- [35] X. Zhu, W. Su, L. Lu, B. Li, X. Wang, and J. Dai, "Deformable detr: Deformable transformers for end-to-end object detection," *arXiv preprint arXiv:2010.04159*, 2020.
- [36] F. Yang, H. Yang, J. Fu, H. Lu, and B. Guo, "Learning texture transformer network for image super-resolution," in *Proceedings of the IEEE/CVF Conference on Computer Vision and Pattern Recognition*, 2020, pp. 5791–5800.
- [37] J. Yu, L. Yang, N. Xu, J. Yang, and T. Huang, "Slimmable neural networks," in *ICLR*, 2019.
- [38] S. Zheng, J. Lu, H. Zhao, X. Zhu, Z. Luo, Y. Wang, Y. Fu, J. Feng, T. Xiang, P. H. Torr, and L. Zhang, "Rethinking semantic segmentation from a sequence-to-sequence perspective with transformers," in *CVPR*, 2021.
- [39] H. Zhang, I. Goodfellow, D. Metaxas, and A. Odena, "Self-attention generative adversarial networks," in *International conference on machine learning*. PMLR, 2019, pp. 7354–7363.
- [40] L. Li and A. Talwalkar, "Random search and reproducibility for neural architecture search," in *UAI*, 2019.
- [41] Z. Guo, X. Zhang, H. Mu, W. Heng, Z. Liu, Y. Wei, and J. Sun, "Single path one-shot neural architecture search with uniform sampling," 2020.
- [42] K. Deb, A. Pratap, S. Agarwal, and T. Meyarivan, "A fast and elitist multiobjective genetic algorithm: Nsga-ii," *EC*, 2002.
- [43] M. Cordts, M. Omran, S. Ramos, T. Rehfeld, M. Enzweiler, R. Benenson, U. Franke, S. Roth, and B. Schiele, "The cityscapes dataset for semantic urban scene understanding," in *CVPR*, 2016.
- [44] S. Ioffe and C. Szegedy, "Batch normalization: Accelerating deep network training by reducing internal covariate shift," *arXiv preprint arXiv:1502.03167*, 2015.
- [45] B. Cheng, "panoptic-deeplab," <https://github.com/bowenc0221/panoptic-deeplab>, 2020.
- [46] R. P. Poudel, S. Liwicki, and R. Cipolla, "Fast-scnn: fast semantic segmentation network," in *BMVC*, 2019.
- [47] X. Li, Y. Zhou, Z. Pan, and J. Feng, "Partial order pruning: for best speed/accuracy trade-off in neural architecture search," in *CVPR*, 2019.
- [48] A. Howard, M. Sandler, G. Chu, L.-C. Chen, B. Chen, M. Tan, W. Wang, Y. Zhu, R. Pang, V. Vasudevan, et al., "Searching for mobilenetv3," in *ICCV*, 2019.
- [49] A. Shaw, D. Hunter, F. Landola, and S. Sidhu, "Squeezenas: Fast neural architecture search for faster semantic segmentation," in *ICCVW*, 2019.
- [50] Q. Wan, Z. Huang, J. Lu, G. Yu, and L. Zhang, "Seaformer: Squeeze-enhanced axial transformer for mobile semantic segmentation," *arXiv preprint arXiv:2301.13156*, 2023.
- [51] B. Zoph, V. Vasudevan, J. Shlens, and Q. V. Le, "Learning transferable architectures for scalable image recognition," in *CVPR*, 2018.
- [52] J. Deng, W. Dong, R. Socher, L.-J. Li, K. Li, and L. Fei-Fei, "Imagenet: A large-scale hierarchical image database," in *CVPR*, 2009.